THE GEOMETRIC SPREADING OF CORONAL PLUMES AND CORONAL HOLES

S. T. SUESS[1], G. POLETTO[2], A.-H. WANG[3], S. T. WU[3] and I. CUSERI[4]
[1]*NASA Marshall Space Flight Center/ES82, Huntsville, AL 35812, U.S.A..*
[2]*Osservatorio Astrofisico di Arcetri, Largo Enrico Fermi, 5, 50125 Firenze, Italy*
[3]*Department of Mechanical Engineering and Center for Space Plasma and Aeronomic Research, University of Alabama, Huntsville, AL 35899, U.S.A.*
[4]*Universitá di Firenze, Firenze, Italy*

(Received 22 September 1997; accepted 18 December 1997)

Abstract. The geometric spreading in plumes and in the interplume region in coronal holes is calculated, using analytic and numerical theoretical models, between 1.0 and 5.0 $R_\odot$. We apply a two-scale approximation that permits the rapid local spreading at the base of plumes (f_l) to be evaluated separately from the global spreading (f_g) imposed by coronal hole geometry. We show that f_l can be computed from a potential-field model and f_g can be computed from global magnetohydrodynamic simulations of coronal structure. The approximations are valid when the plasma beta is small with respect to unity and for a plume separation small with respect to a solar radius.

1. Introduction

The geometric spreading along a stream or flux tube in a coronal hole is generally described in terms of the area, $A(r)$, or the spreading (or expansion) factor, $f(r)$, of a nearly radial, infinitesimal flux tube under steady-flow conditions. In spherical coordinates, where A_0 is the area of the flux tube at its base, at radius r_0, $f(r)$ is defined in terms of $A(r)$ through the equation

$$A(r) = (r/r_0)^2 f(r) A_0. \tag{1}$$

Here we show what theoretical predictions are for the variation of $f(r)$ in coronal plumes and coronal holes.

The interest in $f(r)$ derives from its importance for the dynamics of the expanding solar wind. Kopp and Holzer (1977) introduced the spreading factor formalism to show that the geometric divergence of coronal holes can impose dramatic changes on steady state solutions to the solar wind equations relative to the solutions in which $f(r) = 1$. Recently, the same formalism has been used to model the flow in coronal plumes, in coronal holes between plumes (the 'interplume' flow), and to undertake studies of complex physical processes that are generally beyond the reach of multidimensional MHD models, such as multifluid flows and anisotropic temperatures (e.g., Habbal *et al.*, 1995; Wang, 1994; Hu, Esser, and Habbal, 1997). There have also been recent studies using SOHO instruments that place empirical constraints on $f(r)$ (DeForest *et al.*, 1997; Poletto *et al.*, 1997). What has been absent are theoretical models of coronal spreading factors. This is

Solar Physics **180:** 231–246, 1998.

despite the existence of MHD models which implicitly contain a partial description of the spreading factors, but for which $f(r)$ has not been specifically derived. For this reason, we describe here what we believe are typical theoretical predictions for spreading in coronal plumes and coronal holes between 1.0 and 5.0 $R_\odot$. The immediate purpose is to show what physical models, based on our present understanding of conditions in coronal holes, predict as an appropriate choice for the $f(r)$ in one-dimensional (1D) flow models.

There are two parts to the calculation of $f(r)$. The first is the spreading at the base of plumes, up to heights comparable to the typical plume separation distance, D, where $D \approx 35\,000$ km (Suess, 1982; DeForest *et al.*, 1997). This calculation accounts for the location of plumes over concentrations of magnetic flux relative to the background distribution of flux in the interplume region (DeForest *et al.*, 1997). The flux from these concentrations spreads out with increasing height, as in the spreading above the chromospheric network described by Gabriel (1976), until the field is approximately uniform. Because the magnetic field is relatively strong, this happens by a height comparable to the distance between flux concentrations (Newkirk and Harvey, 1968; Del Zanna, Hood, and Longbottom, 1997). The second part of the calculation is the spreading imposed by the geometry of the coronal holes in which plumes lie. This occurs over a length scale that is large relative to the typical distance between plumes. Therefore, plume spreading is most simply thought of, and can be mathematically approximated as a 'two-scale' problem in which the local spreading at the base of plumes is computed separately from the larger scale spreading defined by the geometry of the coronal hole. This approach can be made formal by assuming the separation can be made and then testing it *a posteriori*, just as done in, for example, boundary layer two scale approximations (Hinch, 1991).

Before calculating $f(r)$, we will describe two general, and basically intuitive results for how the spreading of the plume and interplume regions behave. These derive directly from the observation that the plasma beta, $\beta = (16\pi nkT/B^2)$, is much smaller than unity, $\beta \ll 1.0$, throughout coronal holes, up to heights of at least 5 $R_\odot$. The first result is that the spreading near the base can be computed from a potential field model. This has already been shown by Newkirk and Harvey (1968), Suess (1982), and Del Zanna, Hood, and Longbottom (1997) and needs little or no additional proof. The second is that higher up in coronal holes the geometric spreading factors along streamlines inside plumes and in the adjacent interplume region vary together, so that if the plume area doubles between 2 and 5 $R_\odot$, then so must the interplume area. This follows directly from $\beta \ll 1.0$, but requires additional discussion since the field there is not a potential field.

To demonstrate the important point that $\beta \ll 1$ in coronal holes, consider conditions at the base of plumes, at the top of the transition region at a height of $\sim$ 7000 km above the photosphere. There, B = O[10–100] G (DeForest *et al.*, 1997), T = O[10^6] K, and n_0 = O[10^7–10^9] cm^{-3} (Ahmad and Withbroe, 1977). Therefore, $\beta = 7 \times 10^{-2}$–7×10^{-6} and is easily $\ll 1$. Outside

plumes, in a coronal hole, both the magnetic field and the density are slightly less, $B = \mathrm{O}[5-10]$ G (DeForest *et al.*, 1997), and $n = \mathrm{O}[10^7-10^8]$ cm^{-3} (Ahmad and Withbroe, 1977), so that $\beta = 3 \times 10^{-2}-7 \times 10^{-4}$. Conditions higher up in coronal holes can be estimated by extrapolating inward from solar wind observations. Suess *et al.* (1996) estimate that $\beta \approx 3.0$ at 1 AU from *Ulysses* measurements. Using the constant velocity approximation and taking the temperature to be $T = \mathrm{O}[10^6]$ K gives $\beta \leq \mathrm{O}[10^{-2}]$ at 5 $R_\odot$. Even if the temperature were as high as $\mathrm{O}[10^7]$ K, as reported recently for the proton kinetic temperature by Kohl, Strachan, and Gardner (1996) and Strachan *et al.* (1997), it would still only give $\beta \leq \mathrm{O}[10^{-1}]$ at 5 $R_\odot$. Because β decreases with decreasing height, it can safely be assumed that $\beta \ll 1.0$ below 5.0 $R_\odot$.

The two-scale problem and associated definitions are described in Section 2, the rapid spreading near the base of plumes will be calculated in Section 3, and the spreading in coronal holes and in plumes above the rapid spreading region will be calculated in Section 4, followed by a brief discussion and summary of the results.

2. Two-Scale Analysis

Given the definition of the spreading factor in (1), the magnetic field variation along a nearly radial field line can be written as

$$B(r) = B_0 \left(\frac{R_\odot}{r}\right)^2 \frac{1}{f(r)} . \tag{2}$$

In coronal holes $f(r)$ is often assumed to increase from unity to some number of O[10] by 5 $R_\odot$, and change slowly, if at all, after that (e.g., Kopp and Holzer, 1977; Hu, Esser, and Habbal, 1997)). As described in the Introduction, it is assumed here that there is superimposed on the global coronal hole spreading analyzed in those earlier studies a local spreading at the base of plumes which changes rapidly between the bottom and some height $\delta R_\odot$ that is of the same order as D, the plume separation distance. With this assumption, we can mathematically separate the two scales by making substitution

$$f(r) = f_l(r) f_g(r) . \tag{3}$$

$f_l(r)$ is the *local* spreading below $\delta R_\odot$, varies rapidly at these heights, and is constant above 35 000 km. $f_g(r)$ is the *global* spreading, which varies much more slowly than $f_l(r)$ below 35 000 km.

Using (3), Equation (2) becomes

$$B(r) = B_0 \left(\frac{R_\odot}{r}\right)^2 \frac{1}{f_l(r) f_g(r)} . \tag{4}$$

The solenoidal condition, $\nabla \cdot \mathbf{B}$, then separates into two equations according to the two scales to give

$$\frac{1}{r^2}\frac{\mathrm{d}(r^2 f(r))}{\mathrm{d}r} = f_g \frac{\mathrm{d}f_l}{\mathrm{d}r} = f_g \frac{\mathrm{d}f_l}{\mathrm{d}z}\,, \quad R_\odot \le r \le R_\odot + \delta R_\odot\,, \tag{5a}$$

$$\frac{1}{r^2}\frac{d(r^2 f(r))}{dr} = f_l \frac{1}{r^2}\frac{\mathrm{d}(r^2 f_g)}{\mathrm{d}r}\,, \quad R_\odot + \delta R_\odot < r < \infty\,, \tag{5b}$$

where z is a local Cartesian coordinate defined such that $\mathbf{e}_z \| \mathbf{e}_r$ and $z = 0$ at $r = R_\odot$. Equation (5a) has reduced to the Cartesian form because the thickness of the layer is small compared to its radius of curvature. Therefore the geometry in this thin layer is Cartesian if $\delta R_\odot \ll R_\odot$ and the magnetic field variation across this layer is given by

$$B(z) = B_0 / f_l(z)\,, \tag{6a}$$

while globally the field variation along a nearly radial magentic field line is given by

$$B(r) = B(z = \delta R_\odot)\left(\frac{R_\odot + \delta R_\odot}{r}\right)^2 \frac{1}{f_g(r)}\,. \tag{6b}$$

Now consider how well the magnetic field is simulated by a potential field for $0 \le z \le \delta R_\odot$. This can be evaluated by analyzing the momentum equation as written in dimensionless form (Del Zanna, Hood, and Longbottom, 1997):

$$(\nabla \times \mathbf{B}) \times \mathbf{B} = (\beta/2)[M_0^2 \rho(\mathbf{V} \cdot \nabla)\mathbf{V} + \nabla p + g_0 \rho r^{-2}\mathbf{e}_r]\,, \tag{7}$$

where the quantities have been nondimensionalized against typical coronal base values, (B_0, T_0, n_0), $M_0 = V_0/V_{s0}$ (V_{s0} is the reference sound speed), and $g_0 = \delta R_\odot G M_\odot m_p/(2kT_0 R_\odot^2)$. The ∇ operators have been scaled by $\delta R_\odot$ since the independent variables may change by as much as an O[1] amount across the thin layer at the base of plumes, while the radius in the gravity term is correctly scaled by $R_\odot$. Consequently, (6) takes on a slightly different form than given by Del Zanna, Hood, and Longbottom in that the definition of g_0 involves the ratio $\delta R_\odot / R_\odot$. With this scaling, all of the dimensionless independent variables and operators inside the square brackets in (6) are assured of being O[1] or smaller.

Equation (7) now provides an easy way of estimating the relative importance of the various terms by estimating the values of β, M_0, and g_0. We have already shown that $\beta \ll 1.0$. Since the flow is subsonic below 2–3 $R_\odot$, then $M_0 \ll 1.0$ as well. Finally, $g_0 = $ O[1], so each complete term inside the square brackets in (6), and not just the individual variables and operators, is of O[1] or smaller, showing that the left-hand side of (6) is of O[β]. So, to O[1], $(\nabla \times \mathbf{B}) \times \mathbf{B} = 0$. Since we impose no currents flowing through the lower boundary, the magnetic field

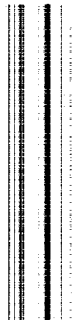

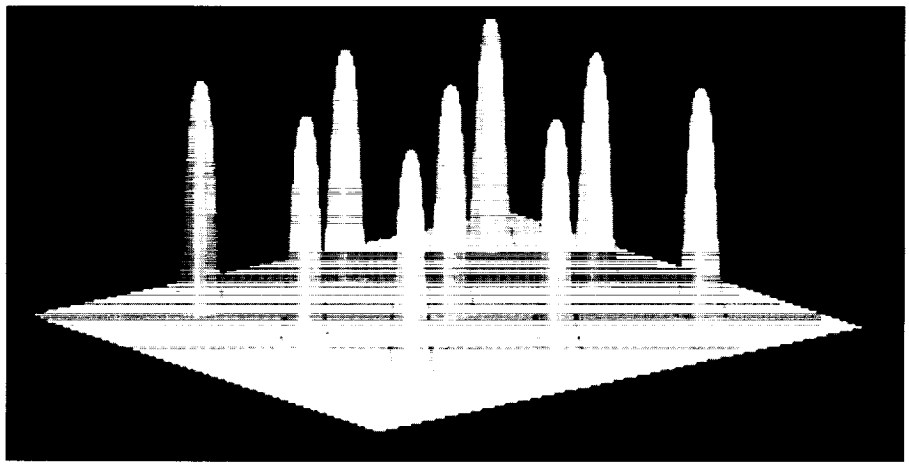

Figure 1. Distribution of flux concentrations on the plane at the base of plumes in the 'mesa' model (see text).

is therefore a potential field to within a formal precision O[β]. This is the point made by Newkirk and Harvey (1968) and Suess (1982). Moreover, Del Zanna, Hood, and Longbottom (1997) demonstrated the validity of the approximation in a quantitative way by showing the small size of first order effects of the presence of a plasma.

3. Spreading at the Base of Plumes

For the present purpose, the important property of the magnetic field at $z = 0$ is that there are quasi-regularly distributed unipolar flux concentrations and a background magnetic field, as most recently found to be the case using MDI observations (DeForest *et al.*, 1997). The example we use has the flux concentrations distributed on vertices of a rectangular grid as given by the expression

$$B_0(x, y) = g(x, y)(1 - c_0) + c_0 \,, \tag{8}$$

where c_0 is a constant giving the ratio of the background average field strength to the peak field strength in the flux concentrations. The function $g(x, y)$ is arbitrary, chosen in such a way as to simulate the shape, areal distribution, and density of magnetic flux concentrations on the $z = 0$ plane. The magnitudes of the field strength and $g(x, y)$ are normalized to unity. An example of $B_0(x, y)$ is shown in Figure 1.

The magnetic field above $z = 0$ can then be shown, using simple potential field theory, to be given by $\mathbf{B} = -\nabla\Phi$, with

$$\Phi = -c_0 z + \sum_{m,n}^{\infty} b_m b_n \exp[-\gamma_{m,n} z] \cos(m\pi x) \cos(n\pi y) \,, \tag{9a}$$

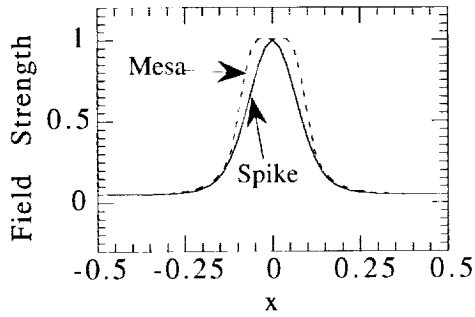

Figure 2. The total magnetic field strength at the base of plumes ($z = 0$) for the 'mesa' and 'spike' distributions.

$$\gamma_{m,n} = \pi(m^2 + n^2)^{1/2} . \tag{9b}$$

This is just the three-dimensional (3D) analog of the 2D calculation described by Suess (1982) (except for the correction in (9b) of a factor of π error that was noted by Del Zanna, Hood, and Longbottom (1997)). The coefficients in (9a) are derived by doing a Fourier decomposition of the flux concentrations using the expression

$$d_{m,n} = \int_0^2 \int_0^2 g(x,y) \cos(m\pi x) \cos(m\pi y)\, \mathrm{d}x\, \mathrm{d}y , \tag{10a}$$

with (for $(m,n) \neq (0,0)$)

$$b_m b_n = \frac{(1 - c_0) d_{m,n}}{\gamma_{m,n}} . \tag{10b}$$

Because this is a potential-field model, the only length scale is the dimensionless ratio of the full width at half-maximum (FWHM) of the flux concentration to the separation between flux concentrations – there is no dimensional scale. Similarly, since the equations are linear in field strength, there is no natural field strength and the only amplitude scale is the ratio c_0. Dimensional values will be introduced later. The field exponentially approaches a smooth value with increasing height, reaching the average value $\bar{g}(1 - c_0) + c_0$ for $z \gg$ the FWHM of the concentration ($\bar{g} \equiv$ the average of $g(x,y)$ over the (x,y) plane). The asymptotic value of the spreading factor can be determined by the percentage of the total flux in the flux concentration and does not require specific evaluation of $f(r)$.

The new calculation we do here is to show the detailed profile of $f_l(z)$, which we do for two cases with different FWHM. These two cases are shown in Figure 2, where the total field strength (Equation (8)) is plotted at the base of the plume along the x-axis (the y-axis is identical). The broader, flatter distribution has a FWHM of ~ 0.14 and the thinner, more peaked distribution has a FWHM of ~ 0.08. In both

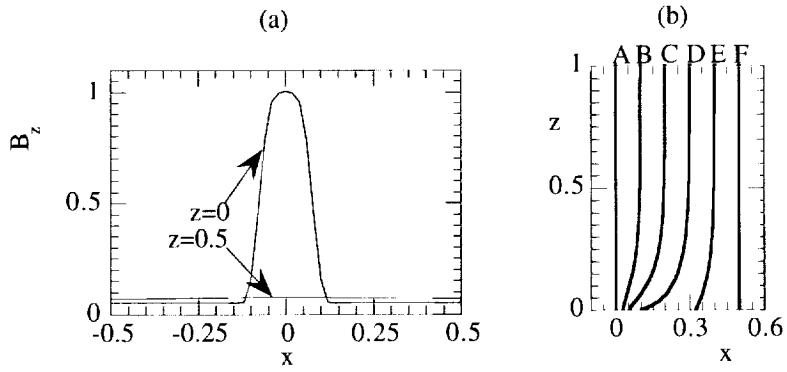

Figure 3. (a) The total field strength at the base ($z = 0$) and at $z = 0.5$ for the 'mesa' model of a plume magnetic flux concentration. The peak to background ratio is 20 at the base but is only 1.05 (5%) at $z = 0.5$. (b) Field lines in the $x - z$ (or $y - z$) plane for the 'mesa' model of a plume.

cases, $c_0 = 0.05$, meaning a 5% background field. We will call these distributions the 'mesa' and 'spike' distributions, respectively, and use them to illustrate the effects of varying shape and FWHM on the solution. The mesa was illustrated in Figure 1.

Equations (9) and (10) were solved for the magnetic field above $z = 0$ and Figure 3(a) shows the resulting field variation at $z = 0.5$ and $z = 0.0$ for the mesa model. It is seen that the field is essentially smooth by $z = 0.5$. As noted in the Introduction, plumes and flux concentrations are typically 35 000 km apart so $z = 0.5$ corresponds to a height of 17 500 km. This meets one of the criteria for the two scale analysis - that the field be smooth by a height $\delta R_\odot \ll R_\odot$ where we will henceforth conservatively take $\delta R_\odot = D = 35\,000$ km. Figure 3(b) graphically shows the shape of the field lines in the x-z plane, illustrating the typical spreading at the base and the rapid approach to nearly vertical field lines by $z = 0.5$ that is implied by the result in Figure 3(a). Note that the field lines are already rapidly diverging at $z = 0$.

The spreading factors are found from Equation (6a) by computing the variation in field strength along a given field line and then dividing that strength by the height. Values are plotted in Figure 4(a) along the field lines labeled A–F in Figure 3(b). The spreading factor has a large positive gradient at $z = 0$, increasing quickly to its maximum value, $f_{l,\max}$, for field lines A–C. Field line C starts at $x \sim 0.15$, well down on the flank of the concentration (see Figure 3(a)), but still reaches approximately the same maximum value of $f_{l,max}$ reached along field lines A and B. Field lines E and F are outside the flux concentration and exhibit values of $f_l(z)$ slightly less than unity, as must be the case for magnetic flux conservation.

The variation of $f_l(z)$ is seen from Figure 4(a) to depend only weakly on position within the flux concentration. Therefore, we can show the characteristic dependence of $f_l(z)$ on FWHM and c_0 by plotting just the variation along field line

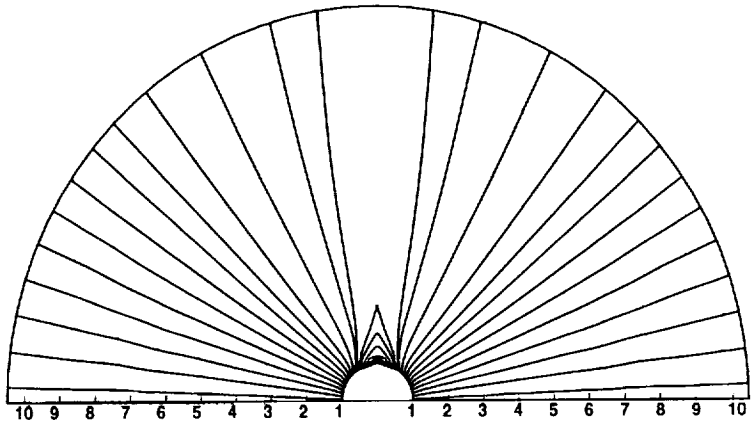

Figure 5. The magnetic field lines in a quasi-steady model for the global MHD structure of the solar corona with a dipolar magnetic field, a momentum and heat sources, and thermal conduction (W97). The axis of symmetry is horizontal and the global topology is similar to that for any model with a heat source. Models without the heat source (SSW, W95) do not have the sharp cusp at the top of the streamer.

relatively slow and dense solar wind which poorly simulates actual coronal hole conditions. W95 is similar to SSW except that $\beta = 1.0$ and it uses a different numerical technique. The density is even higher in the open fields at the poles than in SSW. W97, using the numerical technique of W95, adds heating and momentum sources and thermal conduction. Furthermore, the boundary conditions depend on polar angle. The consequence is that W97 simulates empirical coronal hole densities, temperatures, and flow speeds in the open regions at the poles while still keeping $\beta \approx 0.5$ at the equator, beneath the streamers. The magnetic field lines for W97 are shown in Figure 5, where the field line geometry is similar to that for all models with volumetric heating (Steinolfson, 1988; Suess *et al.*, 1996; Wang *et al.*, 1997). W95 and SSW, without volumetric heating, have more rounded streamers than those shown in Figure 5. The difference is due to the slow expansion of the streamers and leakage of slow solar wind out of the tops of the streamers when there is volumetric heating, a process which is called streamer evaporation (Suess *et al.*, 1996).

The spreading factor, $f_g(r)$, was computed using Equation (6b) along two field lines for each example; one near the center of the open field region ($\theta = 0^o$) and one near the boundary of the streamer. First the coordinates along a magnetic field line were computed from the base of the corona upward from the numerical solution, then the field strength along the line was inserted into (6b) to give $f_g(r)$. Because the streamer width varies between the models, the starting polar angles for the field line near the boundary of the streamer vary. The spreading factors between 1.0 and 5.0 $R_\odot$ are shown in Figure 6.

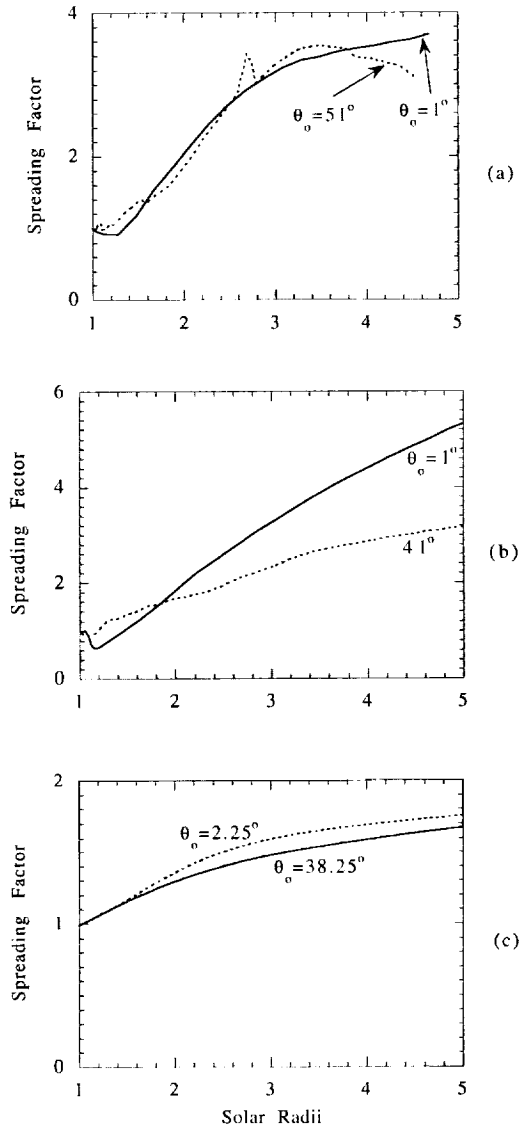

Figure 6. Spreading factors from the MHD global coronal models SSW (a), W95 (b), and W97 (c). These models are described in the text. In each panel, the spreading factor along a field line near the center of the coronal hole ($\theta \leq 2.25°$) is shown as a solid line and that along a field line near the edge of the coronal hole ($\theta \geq 38.25°$) is shown as a dashed line. The indicated angle for each field line is the angle at the footpoint, at $1.0 = R_{\odot}$.

Figure 6 can be summarized by noting that although there are broad similarities between the three models, there are several specific differences. The similarities are that the spreading varies smoothly with radius and $f_{g,\max} \leq 6.0$ in all the cases – although the W95 $\theta = 1°$ result may become larger than 6.0 at larger radii. Potential

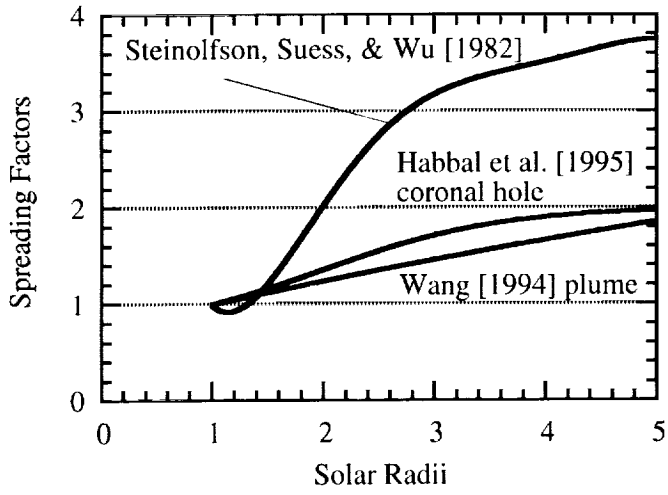

Figure 8. Comparison of the global spreading factor in the $\theta = 1^{o}$ direction from Steinolfson, Suess, and Wu (1982), the plume spreading factor from Wang (1994), and the Habbal *et al.* (1995) interplume spreading factor between 1.0 and 5.0 $R_{\odot}$.

using the exponential variation suggested by Equation (9). This would apply to the spreading in plumes. A corresponding, but much smaller, decrease in $f_I(r)$ to values less than unity should occur in the interplume region in this thin layer at the base of plumes.

A more serious conflict is found in the choice by Habbal *et al.* (1995) of different rates of change for $f(r)$ in the plume and interplume above heights of 35 000 km. The physical arguments and theoretical models described here strongly suggest that the relative changes in the spreading factors should be the same. The choice by Habbal *et al.* (1995) was based on a reported empirical result that the spreading factor in plumes was near unity, based on the observed widths in brightness of plumes using SPARTAN 201 (Guhathakurta and Fisher, 1995). The only explanation for this discrepancy is that the widths in brightness do not necessarily correspond to the width that would be computed by following a specific stream or field line, since the two are not necessarily the same (Suess, 1982).

More generally, the spreading factors utilized in these two 1D models are well within the range of possibilities for $f_g(r)$ derived from global MHD models – the SSW curve for $f_g(r)$ is overlaid onto Figure 8 to illustrate this point. This is reassuring since the numbers used in the 1D models were derived from estimates based on the empirical geometry of boundaries of coronal holes (Munro and Jackson, 1977) which, by the arguments presented here, should be typical of the values throughout coronal holes. It means that the values for $f_g(r)$ derived from all the MHD models are consistent with values derived empirically for large polar coronal holes near sunspot minimum.

6. Summary

The geometric spreading in coronal plumes and coronal holes has been derived here from theoretical models, based on the observation that $\beta \ll 1.0$ throughout coronal holes. The calculations were done in two parts. First the spreading below $\delta R_\odot = D$ was found, where $D = 35\,000$ km is the typical distance between plumes or magnetic flux concentrations lying at the base of plumes (there are probably many more flux concentrations than plumes). This spreading was found using a potential field model. It showed that plume spreading is ~ 15 for a 5% background interplume field and that there is a small corresponding convergence in the interplume region at these heights. The field is then locally smooth above $\delta R_\odot$. Second, it was shown that the global spreading above $\delta R_\odot$ could be calculated using global MHD models and this was done for three different published models. The spreading was determined to be similar to empirical spreading found from the geometry of coronal holes boundaries, $f_{g,\max} \sim 1.5$–6 at 5.0 $R_\odot$. Combining these two results produces an overall spreading in plumes of ~ 40 between 1.0 and 5.0 $R_\odot$, with most of this increase occurring below $\delta R_\odot$.

An important general result is that plume and interplume relative spreading is the same to within a factor of O[β] above $\delta R_\odot$=35 000 km. Plume and interplume spreading differs strongly between plume base and $\delta R_\odot$, over which distance the initially nonuniform magnetic field becomes smooth on transverse scales small compared to a solar radius. However, if a plume area doubles between, (e.g., 1.5 and 5.0 $R_\odot$, then the nearby interplume area will also double over this height (maintaining, of course, any relative differences between the plume and interplume spreading which existed at the height $\delta R_\odot$). This point is made here specifically because there are reported differences in empirical relative spreading between plumes and interplume in this part of the corona. It will be important to understand the source of these differences since the physical premise for the conclusions reported here seems strong.

Acknowledgements

The work of G. Poletto has been partially supported by ASI (Italian Space Agency). The work of S. Suess has been supported by the *Ulysses*/SWOOPS and SOHO/UVCS experiments of NASA and by GNA (National Astronomy Group) of Italy. A.-H. Wang and S. T. Wu have been supported by the Naval Research Laboratory through USRA N00014-C-95–2058 and NASA Grant NAG5-6174.

References

Ahmad, I. A. and Withbroe, G. L.: 1977, *Solar Phys.* **53**, 397.

DeForest, C. E., Hoeksema, J. T., Gurman, J. B., Thompson, B., Plunkett, S. P., Howard, R., Harrison, R., and Hassler, D. M.: 1997, *Solar Phys.* **175**, 393.

Del Zanna, L., Hood, A. W., and Longbottom, A. W.: 1997, *Astron. Astrophys.* **381** (3), 963.

Gabriel, A. H.: 1976, *Phil. Trans. Roy. Soc.* **A281**, 339.

Groth, C. P. T., DeZeeuw, D. L., Marshall, H. G., Gombosi, T. I., Powell, K. G., and Stout, Q. F.: 1997, *EOS* **78** (17), S259.

Guhathakurta, M. and Fisher, R. R.: 1995, *Geophys. Res. Lett.* **22**, 1841.

Habbal, S. R., Esser, R., Guhathakurta, M., and Fisher, R. R.: 1995, *Geophys. Res. Lett.* **22**, 1465.

Hinch, E. J.: 1991, *Perturbation Methods*, Cambridge University Press, Cambridge.

Hu, Y. Q., Esser, R., and Habbal, S. R.: 1997, *J. Geophys. Res.* **102**, 14,661.

Kohl, J. L., Strachan, L., and Gardner, L. D.: 1996, *Astrophys. J.* **465**, L141.

Kopp, R. A. and Holzer, T. E.: 1977, *Solar Phys.* **49**, 43.

Mikić, Z. and Linker, J. A.: 1996, in D. Winterhalter, J. T. Gosling, S. R. Habbal, W. S. Kurth, and M. Neugebauer (eds.), *Solar Wind Eight*, American Inst. of Phys. Conf. Proc. 382, Woodbury, New York, p. 104.

Munro, R. H. and Jackson, B. V.: 1977, *Astrophys. J.* **213**, 874.

Newkirk, G., Jr. and Harvey, J.: 1968, *Solar Phys.* **3**, 321.

Pneuman, G. W. and Kopp, R. A.: 1971, *Solar Phys.* **18**, 258.

Poletto, G., Corti, G., Kohl, J., Noci, G., and Suess, S. T.: 1997, *Bull. Am. Astron. Soc.* **29** (2), 880.

Steinolfson, R. S.: 1988, *J. Geophys. Res.* **93**, 14261.

Steinolfson, R. S., Suess, S. T., and Wu, S. T.: 1982, *Astrophys. J.* **255**, 730.

Stewart, G. A. and Bravo, S.: 1996, in D. Winterhalter, J. T. Gosling, S. R. Habbal, W. S. Kurth, and M. Neugebauer (eds.), *Solar Wind Eight*, American Inst. of Phys. Conf. Proc. 382, Woodbury, New York, p. 145.

Strachan, L., Gardner, L. D., Smith, P. L., and Kohl, J. L.: 1997, in S. R. Habbal (ed.), *Scientific Basis for Robotic Exploration Close to the Sun*, American Inst. of Phys. Conf. Proc. 385, Woodbury, New York, p. 113.

Suess, S. T.:1982, *Solar Phys.* **75**, 145.

Suess, S. T. and Smith, E. J.: 1996, *Geophys. Res. Lett.* **23**, 3267.

Suess, S. T., Wang, A.-H., and Wu, S. T.: 1996, *J. Geophys. Res.* **101**, 19957.

Suess, S. T., Smith, E. J., Phillips, J., and Nerney, S.:1996, *Astron. Astrophys.* **316**, 304.

Wang, A.-H., Wu, S. T., Suess, S. T., and Poletto, G.: 1995, *Solar Phys.* **161**, 365.

Wang, A.-H., Wu, S. T., Suess, S. T., and Poletto, G.: 1997, *J. Geophys. Res.*, in press.

Wang, Y.-M.: 1994, *Astrophys. J.* **435**, L153.